

The Accuracy of an Automasking Algorithm in Plantar Pressure Measurements

Scott J. Ellis, MD · Hill Stoecklein, BS · Joseph C. Yu, BS · Grisha Syrkin, BS · Howard Hillstrom, PhD · Jonathan T. Deland, MD

Received: 19 May 2010/Accepted: 28 September 2010/Published online: 30 November 2010
© Hospital for Special Surgery 2010

Abstract Masking algorithms provide a way to analyze plantar pressure parameters based on distinct anatomical regions of the foot. No study has addressed their accuracy. The purpose of this study was to determine the accuracy of the Novel® ten-region standard masking algorithm in both dynamic and static measurements in normal feet. Static and dynamic plantar pressure measurements were collected from ten normal subjects (20 ft) with and without 10-mm radiopaque markers placed under the first through fifth metatarsal heads, fifth metatarsal base, and first proximal phalanx. The automask was then applied to subdivide the foot into distinct anatomical areas. Weight-bearing AP radiographs were obtained with and without markers. Plantar pressures and radiographs were overlaid. The percent accuracy of each marker within its appropriate mask region was calculated. The average accuracies of the automasking algorithm regions for dynamic and static measurements, respectively, were 98.8% and 90.4% (1MH), 89.9% and 80.6% (2MH), 98.6% and 81.4% (3MH), 96.8% and 82.3% (4MH), 93.1% and 80.8%

(5MH), 97.3% and 92.5% (5MB), and 91.2% and 64.2% (1PPH). Marker presence did not alter foot structure or function as determined by intermetatarsal angles (range, $p=0.361$ to $p=0.649$) and the center of pressure excursion index ($p=0.727$), respectively. The automasking algorithm accurately identifies most foot regions in normal feet, particularly in gait. Such accuracy may be reduced in the setting of foot deformity. Understanding the accuracy of masking algorithms may help guide the interpretation of plantar pressure measurements and ultimately both conservative and operative treatment decisions.

Keywords plantar pressure · anatomical masking · algorithm · accuracy · normal foot · static · dynamic

Introduction

Plantar pressure analysis has emerged as a tool for objectively measuring foot function both in research and clinical arenas and can help guide both conservative and surgical decision-making [10, 23]. Plantar pressure distributions allow visualization of high-pressure areas which many authors believe is a primary risk factor for plantar ulcers in diabetes and other pathologies [6, 25]. Pressure analysis has also been used to characterize foot type [6, 8]. The EMED-X® sensory array, a capacitance-based system in which individual sensors are arranged in a regular matrix [20], represents one increasingly popular method [10, 2–4, 9, 11–13, 29].

A common method of analyzing plantar pressures is to “mask” the foot into anatomical regions of interest to provide more clinically relevant information than when examining the foot as a whole. Masking algorithms can be grouped into two categories [27]. First, the foot can be divided in a geometrical fashion (i.e., a longitudinal bisection into medial and lateral or a horizontal trisection into the hindfoot, midfoot, and forefoot). This approach may not be robust enough to evaluate feet with deformity. Second, an anatomical approach breaks the foot up into specific anatomical areas of interest. The Novel® Multi-

Each author certifies that he or she has no commercial associations (e.g., consultancies, stock ownership, equity interest, or patent/licensing arrangements) that might pose a conflict of interest in connection with the submitted article.

Each author certifies that his or her institution has approved the human protocol for this investigation and that all investigations were conducted in conformity with ethical principles of research, and that informed consent for participation in the study was obtained.

Level of Evidence: Level IV: Diagnostic Study.

S. J. Ellis, MD (✉) · H. Stoecklein, BS · J. C. Yu, BS · G. Syrkin, BS · J. T. Deland, MD
Department of Foot and Ankle Surgery,
Hospital for Special Surgery,
535 East 70th Street,
New York, NY 10021, USA
e-mail: elliss@hss.edu

H. Hillstrom, PhD
Leon Root Motion Analysis Laboratory,
Hospital for Special Surgery,
535 East 70th Street,
New York, NY 10021, USA

mask software (Novel GmbH Munich, Germany) imparts the ability to “automask” the foot into the desired number of regions. Specific plantar pressure variables may be calculated for each individual mask or region. Such automasks have been applied to analyze the plantar pressures during specific activities [19], the effect of surgical reconstruction [22], normal walking parameters [1, 3, 12, 24, 29], and other foot and ankle pathology [4, 5].

One commonly used algorithm is the Novel® ten-region standard automask [21, 29, 3]. Though some data suggests this algorithm is reliable using both the two-step and midgait methods [3], no study to date has assessed its accuracy. Unfortunately, masking inaccuracy potentially limits the conclusions that can be drawn from plantar pressure studies. It is important to understand the accuracy of these widely used algorithms in order to interpret data that may guide both conservative and surgical treatment decisions.

This study sought to assess the accuracy of the Novel® ten-region masking algorithm for dynamic and static measurements in normal feet. Specifically, we hypothesized that the algorithm would accurately identify the metatarsal head regions, the fifth metatarsal base, and the proximal phalanx for both test conditions. Furthermore, we predicted that the percent accuracies would show good to excellent inter-rater reliability for both test conditions. A secondary aim was to demonstrate that parameters of foot function and structure did not change after applying markers to the plantar aspect of the foot needed to test the primary hypothesis. The final aim was to assess the accuracy of the investigator's placement of these plantar markers at specific anatomical foot locations.

Materials and Methods

The study evaluated plantar pressures in a single group of ten healthy subjects (20 ft). All subjects gave informed consent to the work. The seven males and three females who participated had a mean age of 28.9 ± 8.7 years (range, 20–47 years), weight of 76.4 ± 6.7 kg (range, 62.6–88.0 kg), and height of 68.8 ± 3.4 cm (range, 63–75 cm). For inclusion, each foot had to demonstrate normal hindfoot alignment as evidenced by a resting calcaneal stance position between 2° of varus and 2° of valgus [14] and normal forefoot alignment. Patients were excluded if they had any history of injury, trauma, deformity, recurrent pain, or surgery of the foot or ankle on either the right or left extremity.

Plantar pressure data was collected for all subjects in both static posture and dynamic gait using the EMED-X® sensory array (Novel, Munich Germany). For static trials, subjects were instructed to stand barefoot with arms to the side, feet shoulder width apart, and the foot of interest on the array. Three, 30-s static trials were acquired for each foot (sampling rate of 10 Hz). Subjects were then asked to complete three dynamic trials (midgait method) for each foot (sampling rate, 100 Hz).

Eleven polyethylene foam markers (Model Aliplast™ 4E, 10 mm diameter, 3 mm=1/8 in. thickness, Alimed, Dedham, MA, USA) with embedded radio-opaque cross-hatched wires were attached via double-sided adhesive tape to 11 anatomic landmarks of interest on the plantar aspect of the foot (Fig. 1a) by palpation by a practicing foot and ankle surgeon. This included the first through fifth metatarsal heads (1MH, 2MH, 3MH, 4MH, and 5MH), fifth metatarsal base (5MB), first proximal phalanx (1PP), second toe (2T),

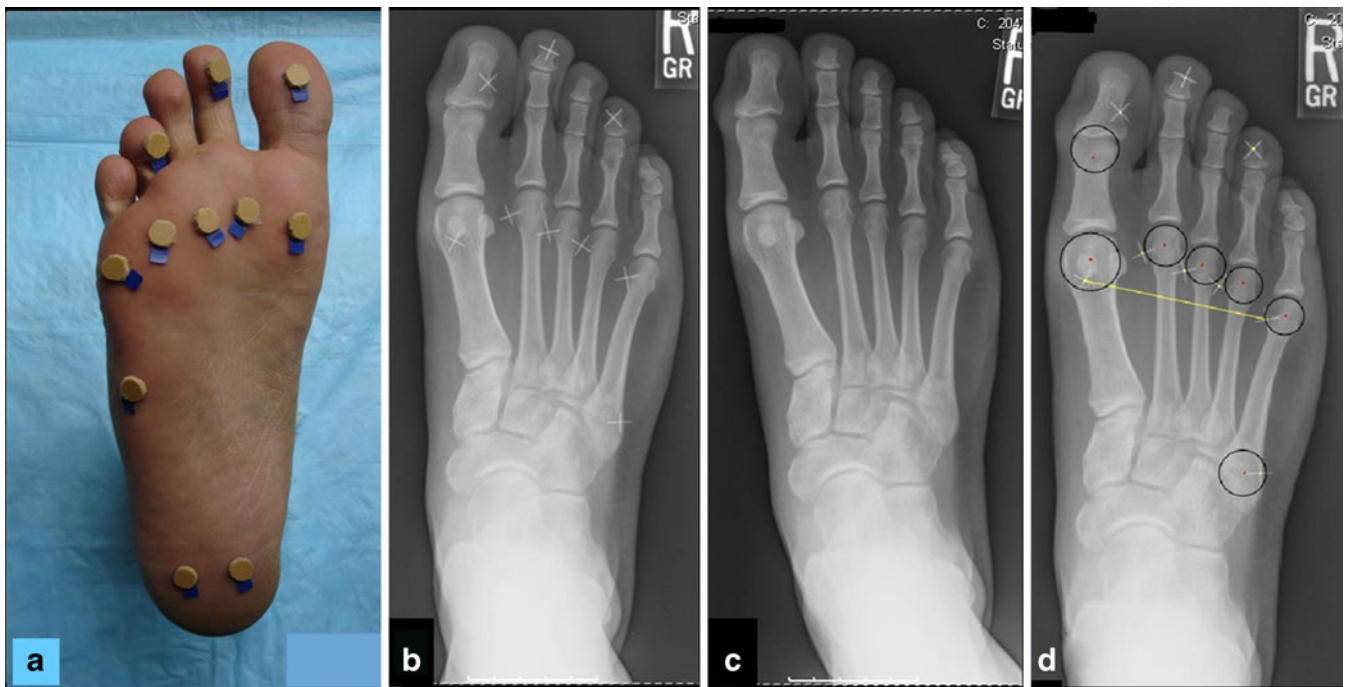


Fig. 1. Markers were secured to the plantar skin over the areas of interest (a). Standard weight-bearing AP radiographs of a foot with (b) and without (c) markers were acquired. Markers can be identified by the embedded wire crosshatches. The centers and circular areas of the

seven anatomic locations (1MH, 2MH, 3MH, 4MH, 5MH, 5MB, and 1PP) used for percent accuracy calculations were identified independently by two raters (d). The intermetatarsal line is drawn between the first and fifth metatarsal heads (yellow line)

fourth toe (4T), medial calcaneus, and lateral calcaneus. With the markers in place, the subjects repeated the three static and dynamic trials per foot in the same manner described above. The markers created a distinct square of four sensors with increased pressure on the plantar pressure images.

With the markers still attached to both feet, weight-bearing AP radiographs were obtained digitally with a Picture Archiving and Communication System (PACS) system. Radiographs of bilateral feet were acquired first with the markers in place and then again after the markers had been removed (Fig. 1b, c). The markers under the medial and lateral calcaneus were obscured by the soft tissue shadow of the hindfoot and were therefore not used in the subsequent steps of the analysis. All images were transferred to digital imaging software (Adobe Photoshop®, Adobe Creative Suite 3 Extended, Adobe, San Jose, CA, USA) for further analysis.

Two experienced raters blindly and independently identified the circular areas and anatomical centers of the metatarsal heads, 5MB, and the head of the 1PP on all radiographic images (Fig. 1d). The osseous borders of the second and fourth toes were outlined in a similar fashion by a single investigator. To minimize potential measurement bias, these identifications were made prior to all other analyses performed by a third investigator.

Standard software (model EMED® X/R, version 19.3.15, Novel, Munich, Germany, and St. Paul, MN, USA) was used to apply a Novel® standard ten-region automasking algorithm to all trials (Fig. 2a). The boundaries between metatarsal regions are defined by this algorithm as distinct percentages of the long plantar angle, defined as that angle formed between the tangents for the medial and lateral sides of the maximum pressure picture (Fig. 2b). No manual alterations were applied to the automask.

Plantar pressure images with masks and digital radiographs for each subject were imported and overlaid on each other within a single image using Adobe Photoshop® (Adobe Creative Suite 3 Extended, Adobe, San Jose, CA, USA). The centers of the four-sensor square area seen on the plantar pressure images were matched to the point of intersection of the wire crosshatches visible on the radiographs for the first and fifth metatarsals (Fig. 3a). The boundaries of the mask were then traced, and the plantar pressure images were removed (Fig. 3b).

The anatomic circles and distal phalanges previously created by the raters were then traced in order to calculate areas using the “lasso tool” (Adobe Photoshop®). The tool was then again used to trace and calculate only that portion of each circle that was located within its appropriate mask region. Area within the appropriate mask region was divided by the total area and multiplied by 100 to obtain the percent accuracy. Each metatarsal head area was checked for its fit within its corresponding metatarsal mask. Percent accuracy for the second toe and combined third, fourth, and fifth toe regions was determined by calculating the percent of the distal phalanx outline that fell within the appropriate mask region. However, because full loading of

the lesser toes rarely occurred during static trials, percent accuracy calculations for these mask regions could be calculated for the dynamic, but not static condition (Fig. 3c, d). Percent accuracy calculations for each anatomical location were averaged across all trials for all feet for both gait and posture conditions.

Potential changes in foot structure caused by the presence of the makers were assessed by comparing radiographic intermetatarsal angles on the AP radiographs with and without markers. Each angle was averaged across all feet. Potential changes in foot function caused by the presence of the markers were evaluated for all dynamic trials using the center of pressure excursion index (CPEI), calculated with standard software (FootAnalNovel, 4.0.5.0, Philadelphia, PA, USA) [26].

The accuracy of the marker placement by manual palpation was assessed by determining the distance (millimeters) on AP radiographs between the crosshatch center of each marker and the anatomical center of the corresponding

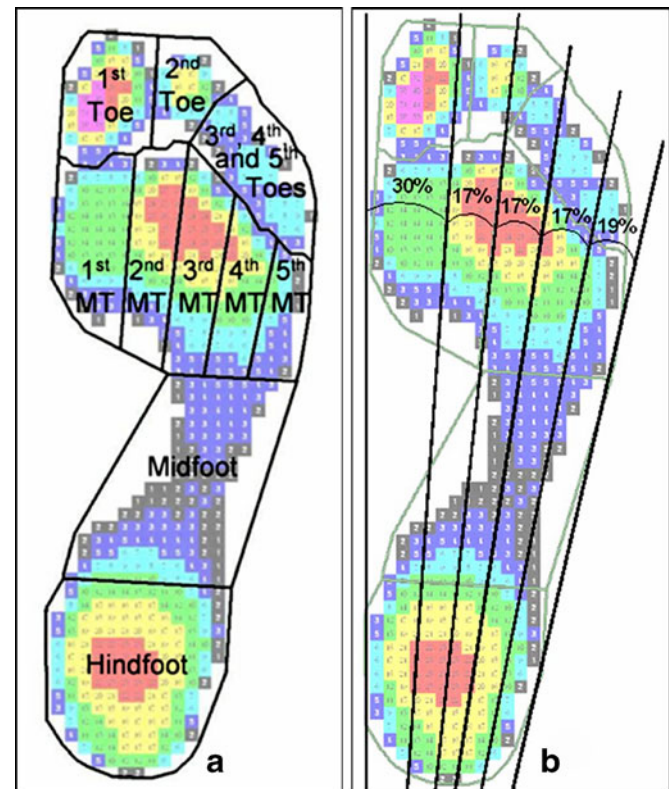


Fig. 2. The Novel® standard ten-region automask was applied to all plantar pressure trials (a). Mask regions include the first toe; second toe; third, fourth, and fifth toes combined; first metatarsal; second metatarsal; third metatarsal; fourth metatarsal; fifth metatarsal; midfoot; and hindfoot. The long plantar angle is defined by the intersection of the medial and lateral borders of the plantar pressure image (b). The metatarsal regions of the automask are defined as 30% (first), 17% (second), 17% (third), 17% (fourth), and 19% (fifth) of the long plantar angle. The boundary between the hindfoot and midfoot is set at 73% of the length from the toes to the heel and the division between the midfoot and forefoot as 45% of the length from the toes to the heel. The boundaries between the forefoot and toes and between the toes themselves are based off the peak pressure values around these areas

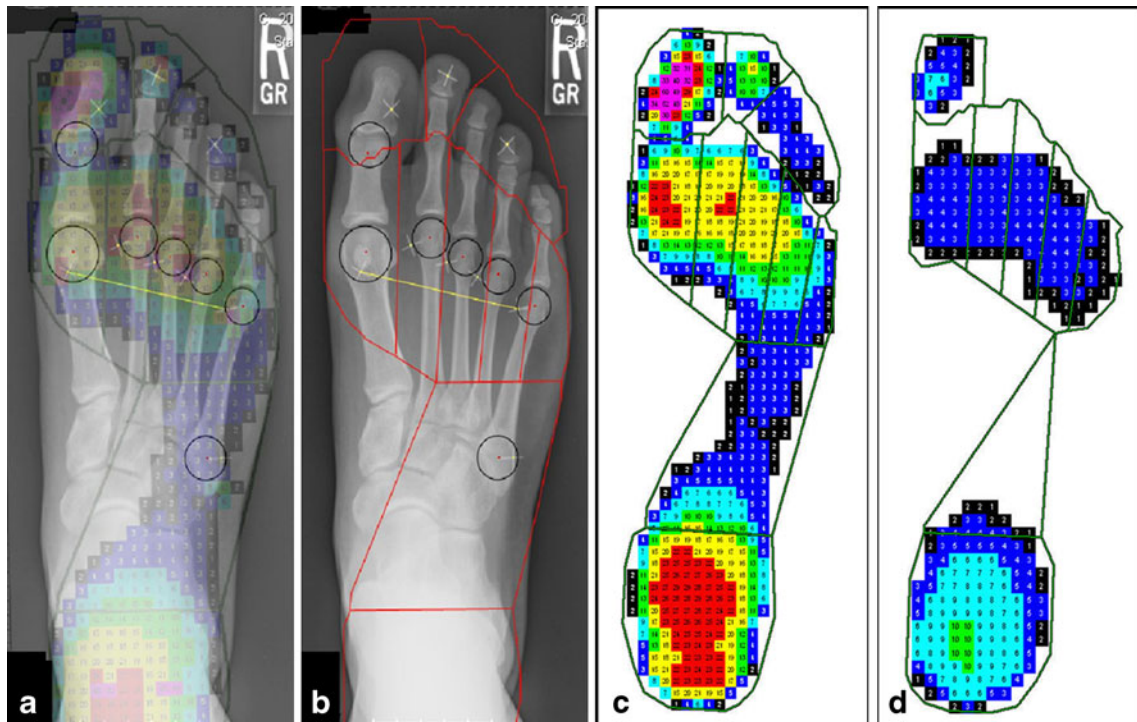


Fig. 3. The radiographs were registered to the plantar pressure images by matching the marker *crosshatch intersection* on the radiograph with the *center of the four sensor areas* of increased pressure on the plantar pressure image for the first and fifth metatarsals (a). Once the images were registered, the automask was traced, and the plantar pressure images were removed. This left the shape of the mask superimposed

on the radiograph (b), after which percent accuracy calculations were carried out. The dynamic (c) and static (d) plantar pressure images illustrate that the lesser toes were most commonly not loaded during static trials, precluding the ability to assess percent accuracy for the second toe and third through fifth toes mask regions

circular area determined by each rater for 1MH, 2MH, 3MH, 4MH, 5MH, and 5MB. Distances were averaged across all feet and calculated separately for each rater using the digital imaging software. The measurements were not calculated for the lesser toe areas because the circular areas and centers of the distal phalanx of interest were not readily identifiable.

Percent accuracy for each anatomical area of interest was calculated for both static and dynamic trials and for both raters. Paired *t* tests were used to compare intermetatarsal angles and CPEI values between conditions with and without markers. The alpha level was set at 0.05.

Results

The automasking algorithm showed high average percent accuracy values across all regions for both raters for dynamic gait (range, 88.7–98.9%; Table 1). All values except for Rater 1 second metatarsal head (88.9%) and Rater 2 first proximal phalanx (88.7%) were greater than 90%. They were highest for the first metatarsal head region (98.7% Rater 1 and 98.9% Rater 2) and lowest for the second metatarsal head for Rater 1 (88.9%) and first proximal phalanx for Rater 2 (88.7%). In general, the percent accuracy in static posture trials was lower for both raters (range, 59.4–92.6%). Values reached 90% or greater only for the first metatarsal head and the fifth metatarsal base and were lowest for the first proximal phalanx (68.9%,

Rater 1 and 59.4%, Rater 2). The percent accuracy for the second toe and combined third, fourth, and fifth toe areas, assessed by only one rater for dynamic trials, averaged 94.8% and 96.1%, respectively.

The radiographic intermetatarsal angles and CPEI demonstrated similar values when testing feet both with and without plantar markers. The average first to second ($p=0.580$), second to third ($p=0.649$), third to fourth ($p=0.361$), and fourth to fifth ($p=0.553$) intermetatarsal angles were statistically similar between the two test conditions. The angles differed by no more than 0.2° . The average CPEI was 18.7 ± 6.5 for feet with markers and 19.5 ± 9.0 for feet without markers (no units, $p=0.727$).

The radiographic distance of the marker crosshatch and the center of the corresponding circular anatomic area was highest for the fifth metatarsal head (6.9 and 6.5 mm for Raters 1 and 2, respectively) and lowest for the second metatarsal head (9.4 and 8.6 mm for Raters 1 and 2, respectively; Table 2). The distance was greater for Rater 1 at all anatomical areas except for the fifth metatarsal base. In all cases, the distance was less than 1 mm.

Discussion

The ten-region standard automasking algorithm accurately identified each metatarsal head, the fifth metatarsal base, the proximal phalanx, and lesser toes in normal feet under the

Table 1 Mean percent accuracy of masking algorithm

	Dynamic		Static	
	Rater 1	Rater 2	Rater 1	Rater 2
1MH	98.7%	98.9%	90.4%	90.4%
2MH	88.9%	90.9%	79.4%	81.7%
3MH	98.4%	98.8%	80.2%	82.5%
4MH	96.5%	97.0%	81.4%	83.1%
5MH	92.6%	93.5%	80.1%	81.5%
5MB	97.4%	97.1%	92.6%	92.3%
1PP	93.7%	88.7%	68.9%	59.4%
Second toe	94.8%	NA	Not calculated	Not calculated
Third, fourth, fifth toes	96.1%	NA	Not calculated	Not calculated

The percent accuracy of each mask region was averaged across all dynamic and static trials and is shown for both raters. The values displayed represent averages of the percent accuracy across all three trials for bilateral feet. The lesser toe regions were only assessed for one rater. Accuracy was not calculated for the lesser toe regions for the static trials because the load placed across the toes was not sufficient. *1MH* first metatarsal head, *2MH* second metatarsal head, *3MH* third metatarsal head, *4MH* fourth metatarsal head, *5MH* fifth metatarsal head, *5MB* fifth metatarsal base, *1PP* first proximal phalanx.

dynamic test condition. Diminished accuracy occurred in the static tests, particularly for the first proximal phalanx. However, the measurement of percent accuracy appeared to be reliable for both test conditions. Foot structure and function did not vary significantly in feet with and without markers, further validating the use of these markers in testing our primary hypothesis. To our knowledge, this is the first assessment of accuracy of the Novel[®] automasking software.

The lower plantar pressure accuracies for static posture trials likely result from the masking algorithm's dependence on sufficient plantar pressure data to construct the medial and lateral plantar angles. The standing condition loads the foot only to a fraction of dynamic walking and may therefore not provide enough contact area for the algorithm to accurately create the mask regions. One must be careful when interpreting the masked data from static posture trials. In addition, it must be noted that posture and gait are very different neuromuscular events [11]. The lower accuracy found in the proximal phalanx, particularly for static trials, is likely due to the fact that it represents a lower loaded area. Why the second metatarsal head was slightly lower than the others is not known. Accuracy may vary from one anatomic area to another and must be considered when drawing conclusions about masked plantar pressure data.

The study is limited by its inclusion of only normal feet, during plantigrade walking and standing, using the EMED-X[®] sensory array and the Novel[®] ten-region standard automask algorithm [21]. Patients with foot malalignment or deformity, particularly those with considerable flatfoot, produce abnormal footprints [17]. The masking algorithm depends on landmarks which may be lacking in the setting of this deformity (i.e., adult-acquired flatfoot, cavovarus foot, and metatarsus adductus) and could preclude accurate identification of certain anatomic regions. The masking

algorithm draws anatomical areas even in the setting of severe deformity such as when patients walk on the inner border, outer border, or even dorsum of the foot. Masks used in these scenarios likely require manual adjustment in order to properly describe the anatomical regions of interest. Most studies utilize plantar pressure masking algorithms to study abnormalities in foot structure or function, not normal plantigrade standing or walking as assessed in the current analysis.

The plantar pressure accuracies found in the current study may differ from those acquired with other in-shoe or custom-made sensor systems which have not been assessed to date [11]. However, good reliability of plantar pressure parameters divided with automasking algorithms with the Novel[®] in-shoe system, Pedar[®], has been shown [15, 16, 18]. Though using similar analyses, different automasking algorithms may give different accuracies.

The distance of the markers from the radiographic centers of the metatarsal heads indicates the inherent difficulty of accurately palpating these landmarks and may result from movement of soft tissue between the markers and bone. These distances and the intermetatarsal angles should be interpreted with caution due to the inherent limitations of using radiographs. There is a certain degree of variability in the two-dimensional projection (i.e., standard radiograph) of a three-dimensional structure (i.e., the foot). Radiographic parameters may vary considerably depending on the position and loading of the foot during the acquisition of the radiograph. Observer or measurement error also introduces variability. Despite these limitations, the data from this study suggests that clinicians should be cautious about the conclusions drawn when examining focal areas of pain or pathology on the plantar aspect of the foot. For example, distinguishing metatarsalgia between adjacent metatarsal heads or from an interspace neuroma may be difficult.

The accuracy data in the current study was limited to the nine regions analyzed, despite using a ten-region automask. This precludes drawing any conclusions with regard to the

Table 2 Mean distance from center of wire crosshatch to center of corresponding landmark of interest

	Rater 1 (mm)	Rater 2 (mm)	Difference in average between raters (mm)
1MH	8.9±4.8	8.1±3.8	0.7
2MH	9.4±2.4	8.6±2.3	0.8
3MH	9.2±2.6	8.3±2.6	0.9
4MH	8.1±2.1	7.6±2.3	0.5
5MH	6.9±2.4	6.5±2.3	0.4
5MB	7.0±3.4	7.5±3.5	0.5

The accuracy of the foam marker placement on the plantar foot was defined as the distance (millimeters) between the point of intersection of the wire crosshatch and the rater-identified anatomical center for the given landmark of interest. The values represent the average distances across all radiographs of bilateral feet with the standard deviation given in parenthesis. Distances were not calculated for the lesser toe regions.

1MH first metatarsal head, *2MH* second metatarsal head, *3MH* third metatarsal head, *4MH* fourth metatarsal head, *5MH* fifth metatarsal head, *5MB* fifth metatarsal base.

heel. Percent accuracy was only calculated for toes in dynamic trials. Though markers were placed on the medial and lateral heel, accuracy was not assessed because the soft tissue shadow of the hindfoot made it difficult to visualize the wire crosshatches on the radiographs. However, because the ten-region mask does not subdivide the hindfoot, it is likely that the relatively small markers would have fallen within the single large hindfoot mask, making analysis less clinically relevant. The two markers were placed on the heel in order to allow future accuracy testing of a 12-region mask which does subdivide the hindfoot. The process was then continued for all subjects for the purpose of consistency. The toes were not loaded sufficiently to perform accuracy assessment in static trials. The distal phalanges were traced for the second and fourth toes because these structures did not contain circular areas and centers that could be easily identified.

Reasonable to good reliability has been shown for multiple parameters taken without masking with the EMED-nt platform using one-step, two-step, and three-step dynamic protocols [28]. Good reliability of the ten-region automask used in the current study has been shown in bilateral feet for several plantar pressure parameters in a group of ten healthy volunteers with the EMED-SF platform [3]. In a separate study using the EMED-AT platform, the midgait method was used to collect plantar pressures on five separate days [12]. Reliability of the ten-region PRC mask [7] was assessed. This algorithm divides the plantar foot into slightly different regions than in the current study. An overall good reliability was discovered for peak pressure, maximum force, impulse, and contact time. However, reliability was better in higher loaded areas of the foot such as the central forefoot. The reliability of masking static posture pressures was not assessed in either study. It is important to understand that reliability may vary for certain plantar pressure variables and anatomic regions and was not assessed in the current study.

In the future, we plan to use a similar process to assess the accuracy of the ten-region automask in patients with adult acquired flatfoot and other types of deformity. This, along with studying accuracy of other masking algorithms, will help clinicians interpret data used both for the purpose of research and surgical decision-making.

In conclusion, the Novel® ten-region standard automask appears to accurately identify anatomic areas of interest in dynamic trials in normal feet. This accuracy diminishes when analyzing static posture data. Such algorithms aid in assessing plantar pressure data for research and clinical purposes. However, caution must be taken when interpreting plantar pressures from posture trials or in feet with deformity.

References

- Bertsch C, Unger H, Winkelmann W, Rosenbaum D. Evaluation of early walking patterns from plantar pressure distribution measurements. First year results of 42 children. *Gait Posture*. 2004;3: 235–242.
- Brophy RH, Gamradt SC, Ellis SJ, Barnes RP, Rodeo SA, Warren RF, Hillstrom H. Effect of turf toe on foot contact pressures in professional American football players. *Foot Ankle Int*. 2009;5: 405–409.
- Bryant A, Singer K, Tinley P. Comparison of the reliability of plantar pressure measurements using the two-step and midgait methods of data collection. *Foot Ankle Int*. 1999;10:646–650.
- Burns J, Crosbie J, Hunt A, Ouvrier R. The effect of pes cavus on foot pain and plantar pressure. *Clin Biomech (Bristol, Avon)*. 2005;9:877–882.
- Bus SA, de Lange A. A comparison of the 1-step, 2-step, and 3-step protocols for obtaining barefoot plantar pressure data in the diabetic neuropathic foot. *Clin Biomech (Bristol, Avon)*. 2005;9: 892–899.
- Cavanagh PR, Rodgers MM, Iiboshi A. Pressure distribution under symptom-free feet during barefoot standing. *Foot Ankle*. 1987;5: 262–276.
- Cavanagh PR, Ulbrecht JS. Clinical plantar pressure measurement in diabetes: rationale and methodology. *Foot*. 1994;123–135.
- Chang CH, Miller F, Schuyler J. Dynamic pedobarograph in evaluation of varus and valgus foot deformities. *J Pediatr Orthop*. 2002;6:813–818.
- Davitt JS, MacWilliams BA, Armstrong PF. Plantar pressure and radiographic changes after distal calcaneal lengthening in children and adolescents. *J Pediatr Orthop*. 2001;1:70–75.
- Ellis SJ, Hillstrom H, Cheng R, Lipman J, Garrison G, Deland JT. The development of an intraoperative plantar pressure assessment device. *Foot Ankle Int*. 2009;4:333–340.
- Firth J, Turner D, Smith W, Woodburn J, Helliwell P. The validity and reliability of PressureStat for measuring plantar foot pressures in patients with rheumatoid arthritis. *Clin Biomech (Bristol, Avon)*. 2007;5:603–606.
- Gurney JK, Kersting UG, Rosenbaum D. Between-day reliability of repeated plantar pressure distribution measurements in a normal population. *Gait Posture*. 2008;4:706–709.
- Kanatli U, Yetkin H, Simsek A, Besli K, Ozturk A. The relationship of the heel pad compressibility and plantar pressure distribution. *Foot Ankle Int*. 2001;8:662–665.
- Keenan AM, Bach TM. Clinicians' assessment of the hindfoot: A study of reliability. *Foot Ankle Int*. 2006;6:451–60.
- Kernozek TW, LaMott EE, Dancisak MJ. Reliability of an in-shoe pressure measurement system during treadmill walking. *Foot Ankle Int*. 1996;4:204–209.
- Kernozek TW, Zimmer KA. Reliability and running speed effects of in-shoe loading measurements during slow treadmill running. *Foot Ankle Int*. 2000;9:749–752.
- Ledoux WR, Hillstrom HJ. The distributed plantar vertical force of neutrally aligned and pes planus feet. *Gait Posture*. 2002; 1:1–9.
- Murphy DF, Beynon BD, Michelson JD, Vacek PM. Efficacy of plantar loading parameters during gait in terms of reliability, variability, effect of gender and relationship between contact area and plantar pressure. *Foot Ankle Int*. 2005;2:171–179.
- Nagel A, Fernholz F, Kibele C, Rosenbaum D. Long distance running increases plantar pressures beneath the metatarsal heads: A barefoot walking investigation of 200 marathon runners. *Gait Posture*. 2008;1:152–155.
- Nicol K, Hennig EM. Measurement of pressure distribution by means of a flexible large surface mat. In: Asmussen E, Jorgenson K, eds. *Biomechanics*. IVA ed. Baltimore: University Park Press; 1978:374–380.
- Novel gmbh. *Novel Scientific Manual*. 12.3rd ed. Munich, Germany: Novel gmbh; May 2004.
- Oeffinger DJ, Pectol RW, Jr, Tylkowski CM. Foot pressure and radiographic outcome measures of lateral column lengthening for pes planovalgus deformity. *Gait Posture*. 2000;3:189–195.
- Richter M, Frink M, Zech S, Vanin N, Geerling J, Droste P, Krettek C. Intraoperative pedography: A validated method for static intraoperative biomechanical assessment. *Foot Ankle Int*. 2006;10:833–842.
- Segal A, Rohr E, Orendurff M, Shofer J, O'Brien M, Sangeorzan B. The effect of walking speed on peak plantar pressure. *Foot Ankle Int*. 2004;12:926–933.

25. Singh N, Armstrong DG, Lipsky BA. Preventing foot ulcers in patients with diabetes. *JAMA*. 2005;2:217–228.
26. Song J, Hillstrom HJ, Secord D, Levitt J. Foot type biomechanics. comparison of planus and rectus foot types. *J Am Podiatr Med Assoc*. 1996;1:16–23.
27. Stebbins JA, Harrington ME, Giacomozzi C, Thompson N, Zavatsky A, Theologis TN. Assessment of sub-division of plantar pressure measurement in children. *Gait Posture*. 2005;4:372–376.
28. van der Leeden M, Dekker JH, Siemonsma PC, Lek-Westerhof SS, Steultjens MP. Reproducibility of plantar pressure measurements in patients with chronic arthritis: A comparison of one-step, two-step, and three-step protocols and an estimate of the number of measurements required. *Foot Ankle Int*. 2004;10:739–744.
29. Wearing SC, Urry SR, Smeathers JE. Ground reaction forces at discrete sites of the foot derived from pressure plate measurements. *Foot Ankle Int*. 2001;8:653–661.